NASA CONTRACTOR REPORT

NASA CR-1301

INVESTIGATION OF A COILABLE LATTICE COLUMN

by R. F. Crawford

Prepared by

ASTRO RESEARCH CORPORATION
Santa Barbara, Calif.
for

NATIONAL AERONAUTICS AND SPACE ADMINISTRATION • WASHINGTON, D. C. • MAY 1969

NASA CR-1301

INVESTIGATION OF

A COILABLE LATTICE COLUMN

By R. F. Crawford

Issued by Originator as Report No. ARC-R-310

Prepared under Contract No. NAS 7-427 by
ASTRO RESEARCH CORPORATION
Santa Barbara, Calif.

for

NATIONAL AERONAUTICS AND SPACE ADMINISTRATION

For sale by the Clearinghouse for Federal Scientific and Technical Information
Springfield, Virginia 22151 – CFSTI price $3.00

INTRODUCTION AND SUMMARY

A lattice column consisting of six longerons interconnected by crossed helical braces was fabricated and tested to determine the feasibility of its concept and to verify analysis of its structural performance. Its helical braces form a cross-sectional shape which can be elastically flattened. This flattened column can then be coiled longitudinally into a relatively small cylindrical volume.

The test segment of the column was fabricated of 0.035-inch diameter steel wires joined together with "coins" into which the intersection of the wires was soldered. Tests were performed on the segment to determine its torsional stiffness, axial buckling strength, and its capability to be flattened and coiled.

Following are the results of the tests:

1. The method used to fabricate the test segment produced a satisfactory model for this exploratory investigation; however, other fabrication methods may prove to be more practicable.

2. The results of several torsional stiffness tests of the column compared well with a theoretical value of 1275 lb-in.^{2} Local buckling of the longerons of the column occurred at a load of 12 pounds. This buckling load is 1.72 times the Euler load for longerons whose ends are hinged. The helical braces stabilized the longerons of the present test segment.

The agreement between theoretical and experimental values of torsional stiffness and buckling load is considered satisfactory for present purposes.

LIST OF SYMBOLS

A, B, C, D, and E	Coefficients of terms in complete solution to differential equation
d_b, d_ℓ	Diameters of brace and longeron elements, respectively
EI	Bending stiffness of either longeron or brace elements
GJ_{EXP}	Experimentally determined torsional stiffness of column
GJ_{THEOR}	Theoretically determined torsional stiffness of column
H	Amplitude of initial shape of brace elements
h	Distance between intersections of brace elements
K	Coefficient in Eq. (15); accounts for effect of braces in stabilizing longerons against local buckling.
L	Column length
ℓ	Length of longeron elements between intersections
M(x)	Internal moment in brace at any position
M_o	Moment required to prevent rotation of one end of brace
P_{CR_C}	Critical buckling load of column
P_{CR_ℓ}	Critical buckling load of one longeron
Q	Axial load in brace due to torsion of column
Q_{EU}	Euler buckling load of brace

Q_{CR}	Critical buckling load of brace
R_c	Top view radii of column cross section
R_p	Packaged radius to which the column is coiled
S	Stiffness of braces under axial loading, Q
S_ℓ	Rotational stiffness which the braces provide in stabilizing the longerons against buckling
T	Torque applied to column
V	Internal reaction force in column due to applied torque
x,y	Coordinate axes for stiffness analysis of braces
$\bar{x}$	Normalized coordinate, $\bar{x} = \frac{x}{h}$
y_o	Initial shape of helical brace
y_Q	Change in shape of brace due to application of axial load, Q
α	Helix angle of braces
λ	Parameter, $\lambda^2 = \frac{Q}{EI}$
δ	Net relative end displacement of brace
δ_V	End displacement of brace in direction of force, V
θ	Twist of column per unit length due to applied torque, T
ϵ_{b_c}	Direct strain in brace due to coiling of column

ϵ_{b_f}	Direct strain in brace due to flattening the column
ϵ_{ℓ_c}	Direct strain in longeron due to coiling the column
γ_{b_f}	Shearing strain produced in a brace due to flattening the column
γ_{b_c}	Shearing strain produced in a brace due to coiling the column

DESIGN CONCEPT

The design concept for this coilable lattice column is illustrated by Figure 1. Longerons are the primary load-carrying members of the structure. The functions of the helical braces are to interconnect, deploy, and stabilize the longerons and to provide the composite structure with shearing and torsional stiffness. The particular number of longerons and the helix angle of the braces shown in Figure 1 are not germane to the concept; they can be optimized in future design studies. The braces are formed of circular arcs of equal radii, assembled in the form shown, so that the maximum normal and shearing strains in the battens resulting from flattening the column are limited to

$$\epsilon_{b_f} = \pm \frac{d_b}{2R_c} \cos^2\alpha \tag{1}$$

$$\gamma_{b_f} = \pm \frac{d_b}{2R_c} \sin\alpha \cos\alpha \tag{2}$$

When the flattened column is then coiled into a cylindrical configuration, the maximum strains in the longerons are

$$\epsilon_{\ell} = \pm \frac{d_{\ell}}{2R_p} \tag{3}$$

This coiling will produce additional normal and shearing strains in the braces, the maximum values of which are

$$\epsilon_{b_c} = \pm \frac{d_b}{2R_p} \sin^2\alpha \tag{4}$$

$$\gamma_{b_c} = \pm \frac{d_b}{2R_p} \sin\alpha \cos\alpha \qquad (5)$$

The structural dimensions to be used for this type of column will depend upon the elastic strain limitations of its material, the structural capabilities required of it, and package size limitations.

TEST SEGMENT

Since the objective of the present investigation is to determine feasibility of the concept and its mechanical properties, the proportions of the test segment were selected only from considerations of fabrication convenience and the requirement that the cross section be flattenable without exceeding the elastic strain limit of the brace material.

A photograph of the test segment is shown in Figure 2. Both the longerons and helical braces were fabricated from 0.035-inch diameter steel music wire, which conforms to MIL-6101 and QQ-W-470-A. The yield strength of the wire is approximately 165 000 psi, and its modulus was determined as 28×10^6 psi. Following is a summary of the dimensions of the test segment.

$$L = 20.9 \text{ in.}$$

$$\ell = 4.18 \text{ in.}$$

$$R_c = 2.00 \text{ in.}$$

$$d_\ell = d_b = 0.035 \text{ in.}$$

$$\alpha = \pi/4 \text{ rad}$$

The helical sections were bent to the required 4-inch radius prior to assembling the column. The ends of the wires were then inserted into the coins on an assembly jig, where they were soldered in place.

The coin-like intersection fittings shown in Figure 3 were made of brass. As indicated, the holes in the thinner coins used for joining longeron intersections are coplanar to avoid eccentricities.

The holes in the thicker coins could not be coplanar. However, eccentricities in these coins, which only connect helical members along the column edges, are not detrimental.

End plates for distributing the applied axial and torsional loads to the members of the column were attached by short wire segments, as indicated in Figure 2.

TEST PROCEDURE AND RESULTS

Torsion Test

Torsional stiffness tests were performed in an apparatus which is shown schematically in Figure 4. The resulting torque-twist data are shown in Figure 5. Nonlinearity and scatter is noted to exist in the data. The nonlinearity appeared to be elastic because no permanent deformations were observed to result from the tests. During application of the torques, the longerons remained unbent. The helical braces underwent increases and decreases in their radii of curvature, depending on their curvature and on whether they were in the directions to resist the applied torque by compression or tension.

The scatter among the various torsion tests shown in Figure 5 was due, at least partially, to variable friction in the test apparatus. The initial slope of the lowest test run gives the following value of the torsional stiffness of the column:

$$\overline{GJ}_{EXP} = 1100 \text{ lb-in.}^2$$

Buckling Test

The test segment was axially compressed as shown by the photograph of the apparatus (Fig. 6). Spherical balls between the segment and the loading apparatus ensured uniform loading of the longerons. Weights were placed on the loading pan of the apparatus in one-pound increments until buckling was observed. The test apparatus was adjusted prior to the test such that the loading pan could travel only 1/16 inch when buckling occurred. Bending of the longerons due to buckling was thus restricted, as is evident in Figure 6, and resulted in no permanent deformations.

The critical load for buckling in the mode shown in Figure 6, the only mode observed, was 12 pounds. The buckling mode was predominantely one in which the intersections of the longerons remained undeflected and the longerons displaced radially inward and outward between intersections, i.e., local Euler buckling of the longerons. The braces restrained rotation of the longeron intersections, as is clear from the analysis of the data given later in this report.

Flattening and Coiling Tests

The test segment was flattened between two transparent plates as shown in Figure 7, and also locally coiled to a radius of approximately 2 inches as shown in Figure 8. No resulting permanent deformations were observed. Coiling to a 2-inch radius would impose a maximum strain of 0.00875 on the longerons or a maximum elastic stress of 242 000 psi. Some question exists as to whether that strain exceeds the elastic limit of the material; therefore unobserved permanent deformations may have resulted.

ANALYSIS OF MECHANICAL BEHAVIOR

Torsional Stiffness

Torque acting on the column may be reacted by forces, $2V$, acting at four typical intersections of the helical braces and in the directions of straight lines between the ends of the braces, as shown in Figure 9. The torque is then related to the reaction forces by

$$T = 4\sqrt{3}\, VR_c \tag{6}$$

Forces, Q, directed along straight lines between the ends of the helical segments equilibrate the intersection forces according to

$$Q = \frac{V}{\cos\alpha} \tag{7}$$

The forces on the helical segments are compression in one half and tension in the other.

The axial stiffness of the braces is derived in the Appendix as follows for values of Q very much smaller than that for Euler buckling of the braces:

$$\frac{Q}{\delta} = \frac{5\ EI}{H^2\ h} \tag{8}$$

In this equation δ is the relative displacement of the ends of a brace when acted upon by force, Q; EI is the bending stiffness of the brace; H is the amplitude of the initial shape (circular) of the brace; and h is the distance between the ends of one brace element.

For the test segment,

$$h = \frac{R_c}{\cos\alpha} \tag{9}$$

and the heights of the circular arcs between intersections are expressed as

$$H = R_c \left(1 - \frac{\sqrt{3}}{2}\right) = 0.134\ R_c \tag{10}$$

In the Appendix, the circular arc shape of the brace was approximated as a segment of a parabola of the same arc height.

Displacements in the direction of forces, V , are related to those in the direction of forces, Q , by

$$\delta_V = \frac{\delta}{\cos\alpha} \tag{11}$$

And, the twist of the column, θ , per unit length is related to δ_V by

$$\theta = \frac{3\ \delta_V}{\pi\ R_c^2\ \tan\alpha\ \cos 30^\circ} \tag{12}$$

By combining Equations (6) through (12), the torsional stiffness of the column, GJ , is found as

$$GJ_{THEOR.} = \frac{T}{\theta} = \frac{10\pi}{(0.134)^2}\ EI\ \cos^2\alpha\ \sin\alpha \tag{13}$$

For the column tested, α was $\pi/4$ and the EI of the braces is calculated as 2.06 lb-in.^{2}. The torsional stiffness of the test column is thus calculated to be

$$GJ = 1275 \text{ lb-in.}^2$$

As shown in Figure 5, this theoretical value compares fairly well with the experimental results.

Buckling Strength

The buckling strength of the column is six times the buckling strength of an individual longeron segment of the column

$$P_{CR_c} = 6\ P_{CR_\ell} \tag{14}$$

The buckling strength of an individual longeron whose ends (intersections with the braces for the test specimens) are elastically restrained against rotation is*

$$P_{CR_\ell} = \frac{K\pi^2\ EI}{\ell^2} \tag{15}$$

The factor, K , in this formula depends on the magnitude of the elastic restraint. Since the experimentally observed value of P_{CR} is 12.0 pounds, and

$$\frac{\pi^2\ EI}{\ell^2} = 1.165 \tag{16}$$

---

* Flugge, W.: Handbook of Engineering Mechanics, McGraw Hill Book Co., Inc. 1962, p. 27 of Sec. 44

for the longerons of the test segment, then

$$K = 1.72 \tag{17}$$

This value of K corresponds* to a longeron end restraint against rotation of 0.271 in.-lb/rad, apparently provided by the helical braces.

*Ibid. page 13

CONCLUSIONS

This investigation has shown that the concept of a coilable lattice column is entirely feasible. Further theoretical and experimental investigations should be performed to define the most suitable proportions as they will vary with loading index, packaging requirements, and material capabilities.

The correlation obtained between experimental and theoretical values of both torsional stiffness and buckling strength is considered to be satisfactory evidence that the mechanics of this concept are understood.

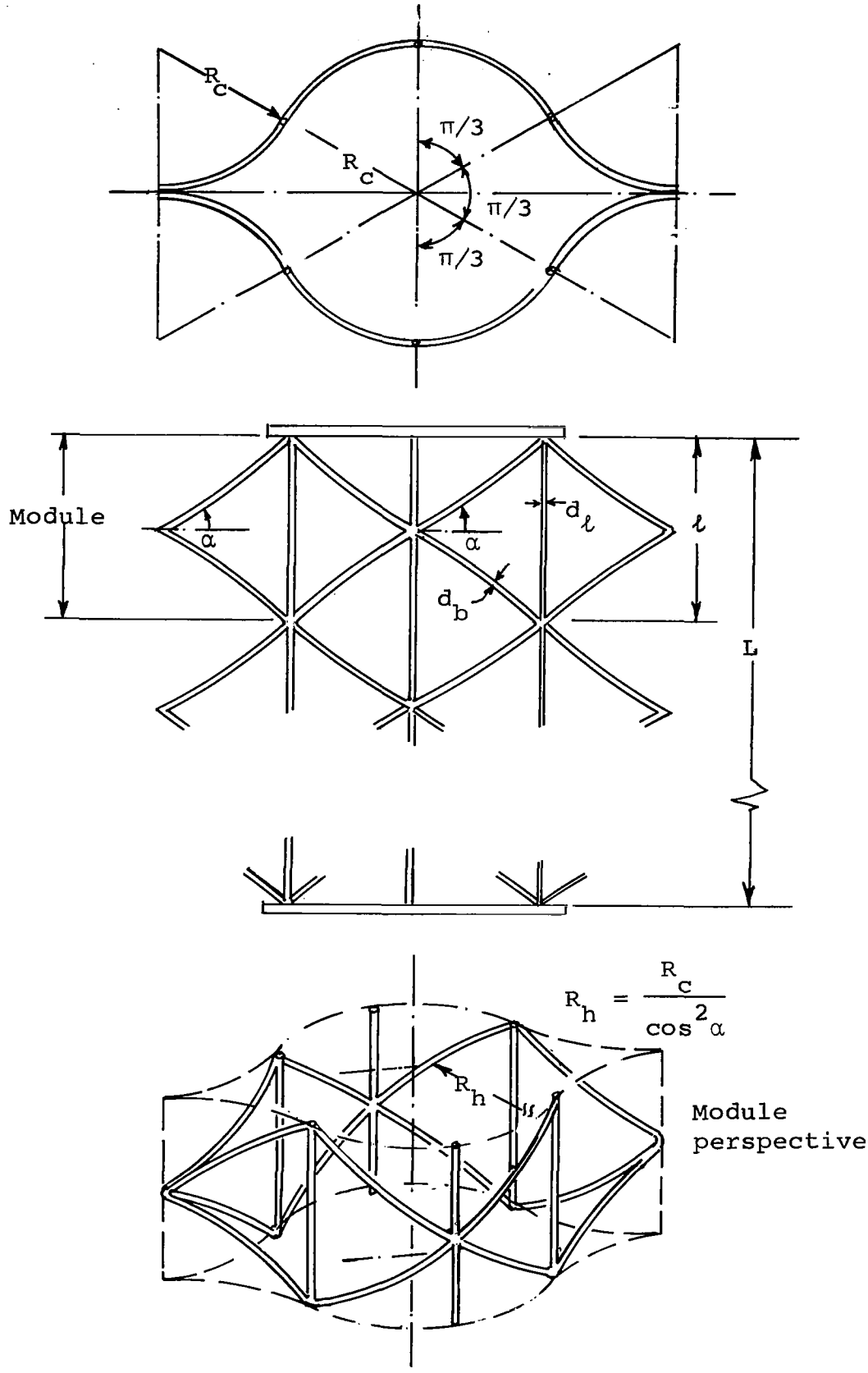

Figure 1. Design Concept of a Coilable Lattice Column

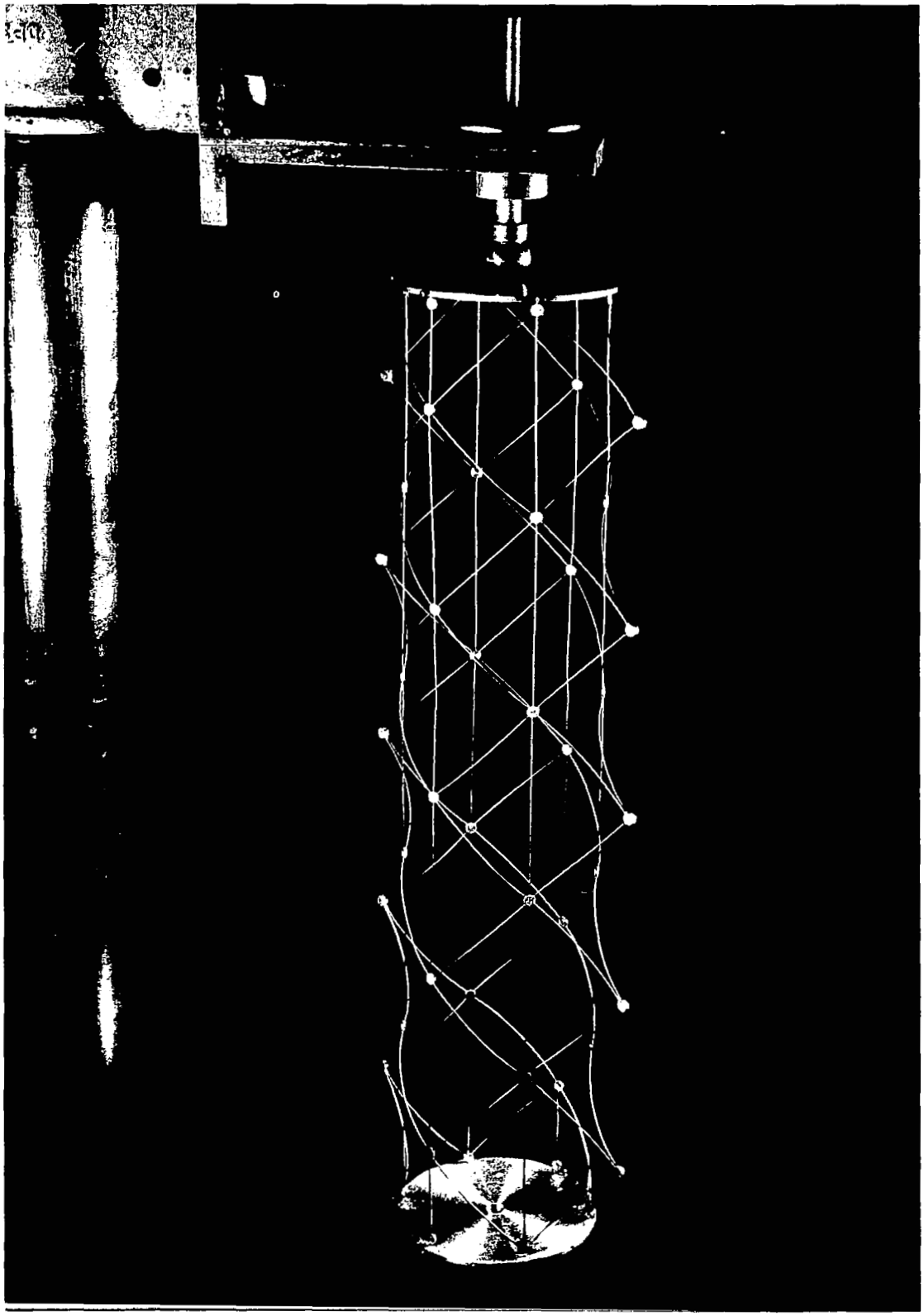

Figure 2. Test Segment of a Coilable Lattice Column

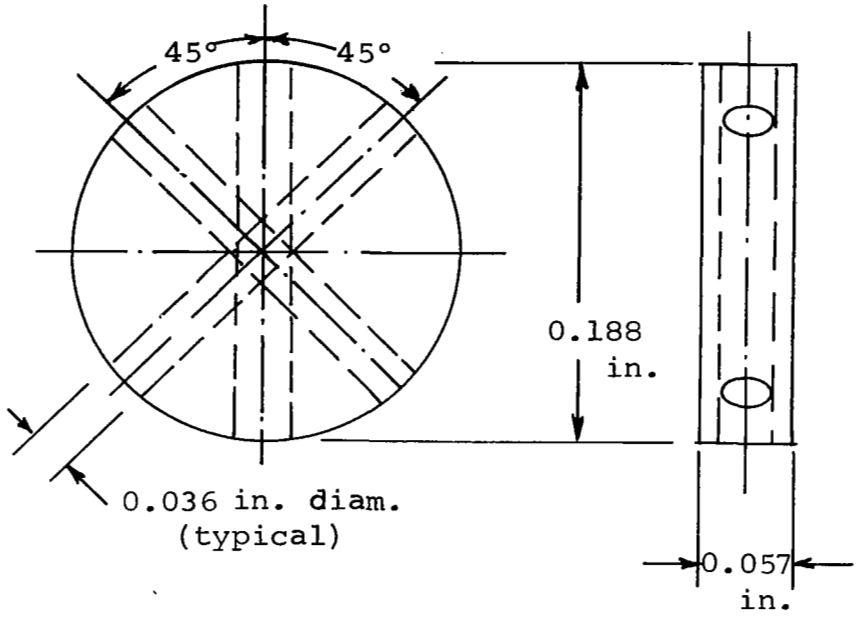

a. Coin for joining intersections of longerons and helical braces

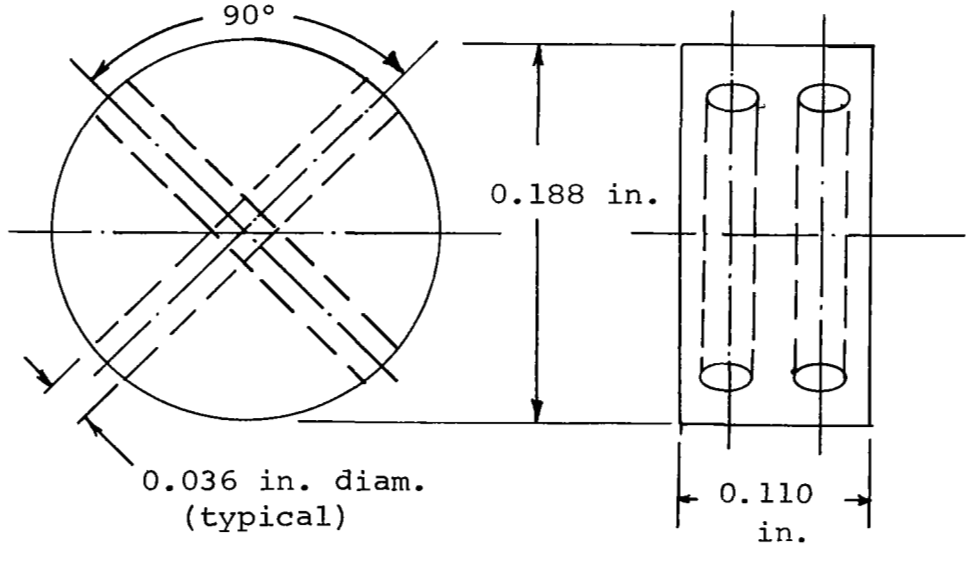

b. Coin for joining braces along edge of column where no longerons are present

Figure 3. "Coins" for Joining Members of Test Segment

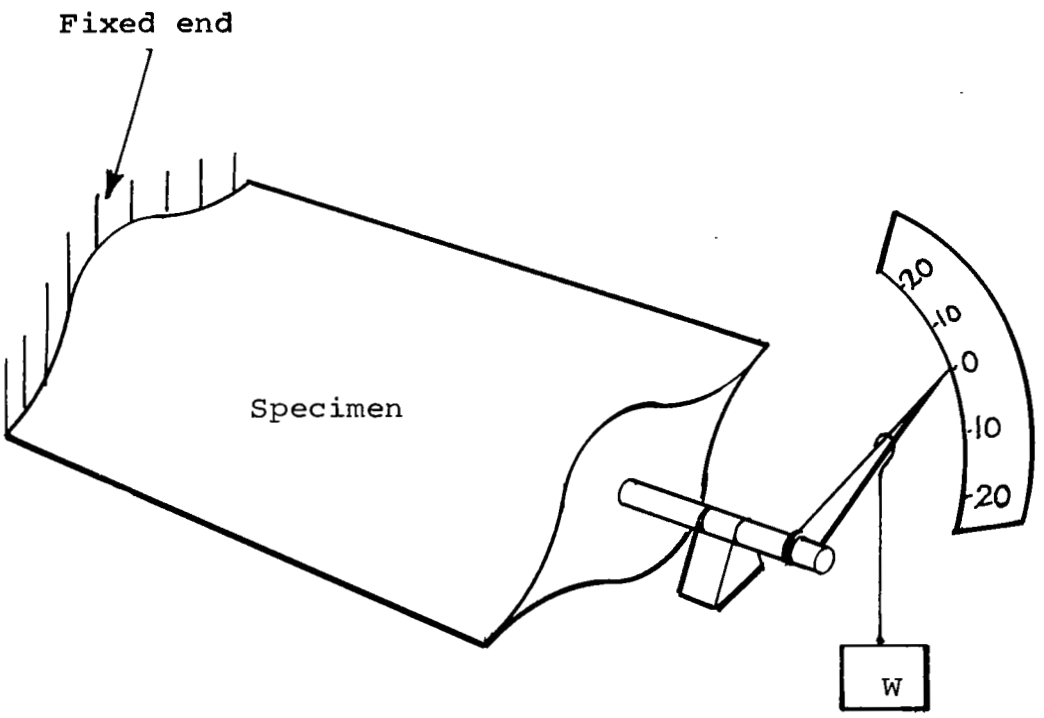

Figure 4. Schematic of Torsional Test Apparatus

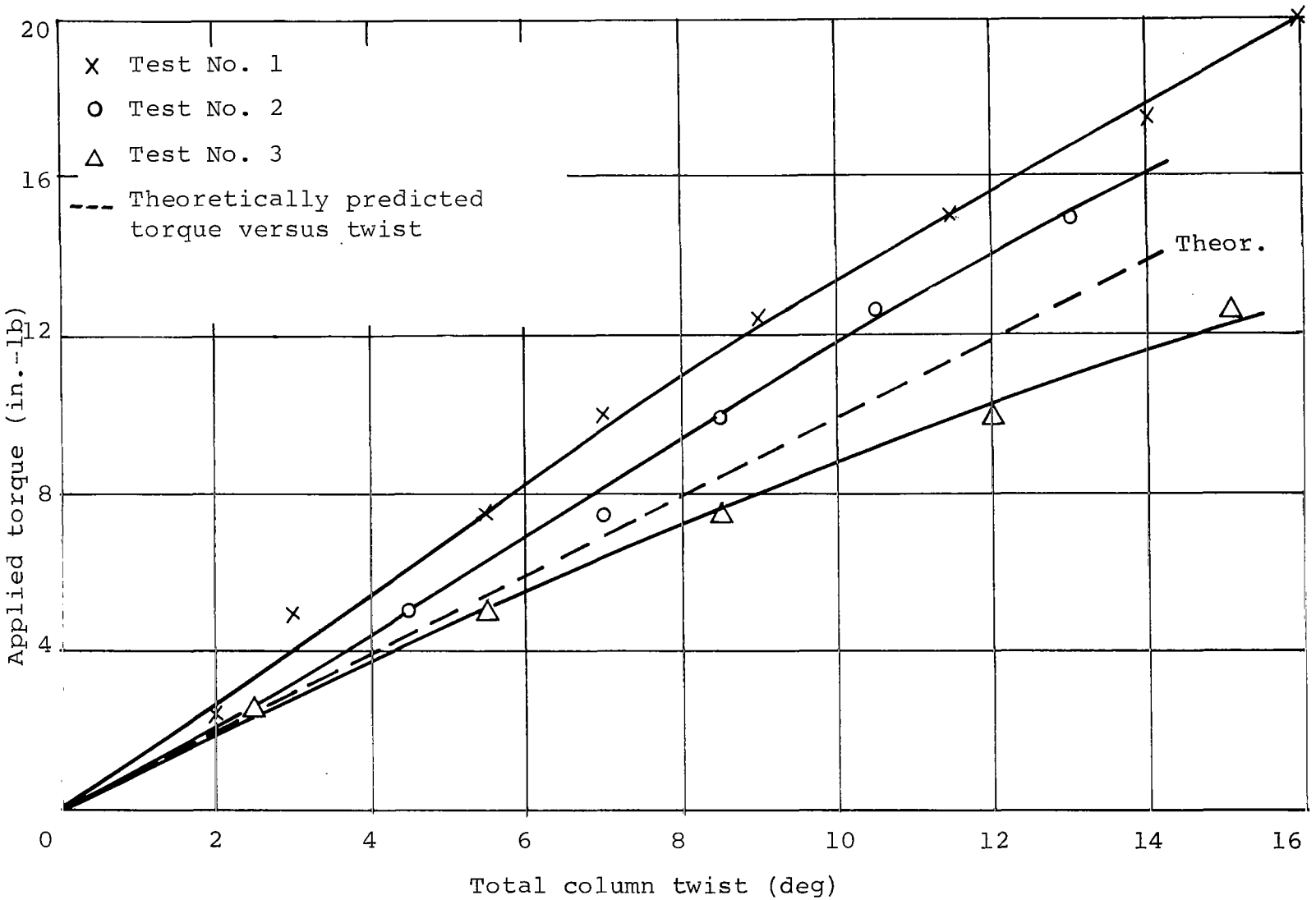

Figure 5. Experimental Values of Torque versus Twist for Three Different Tests Compared with Theoretical Values

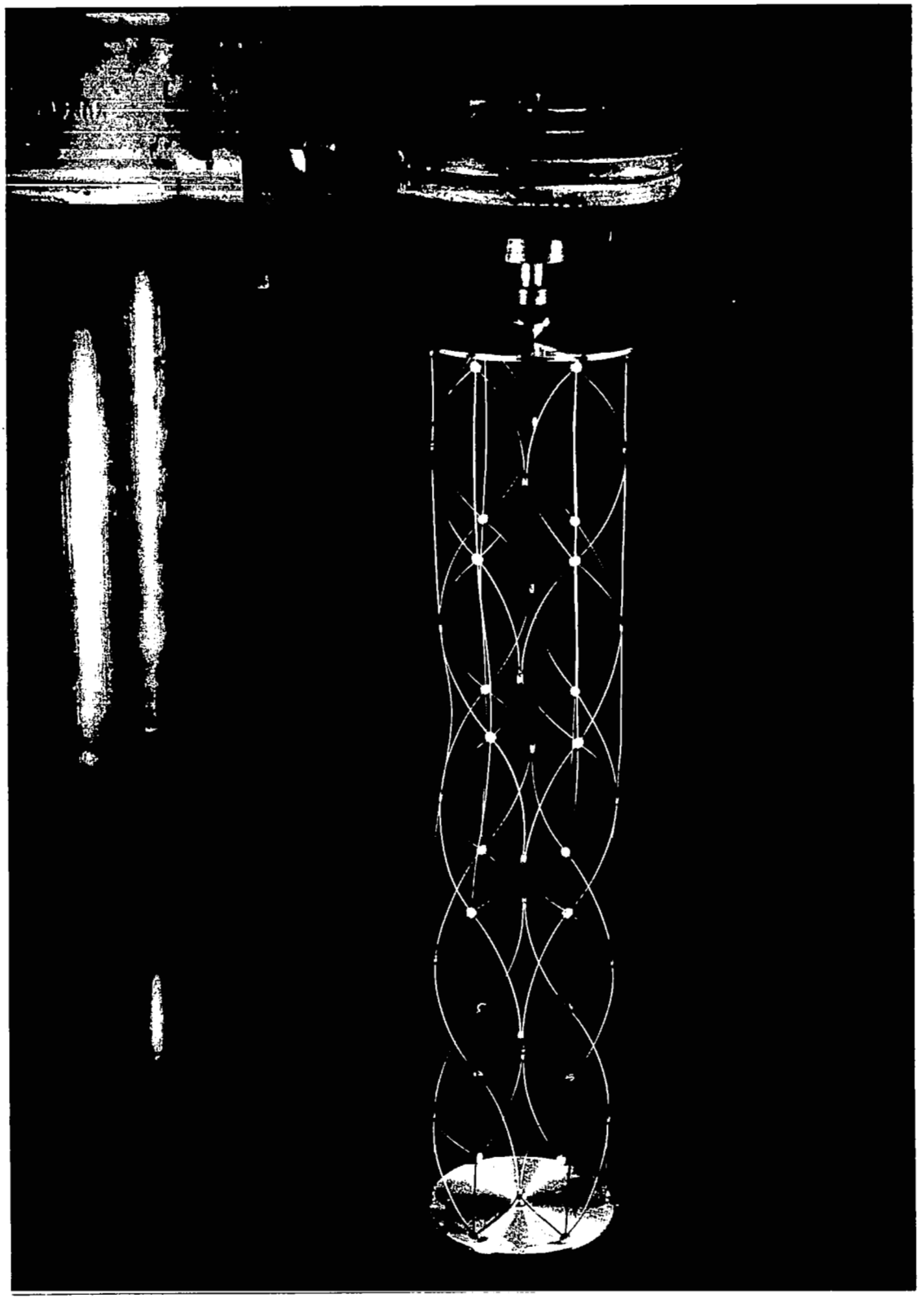

Figure 6. Test Segment as Buckled by Axial Compression

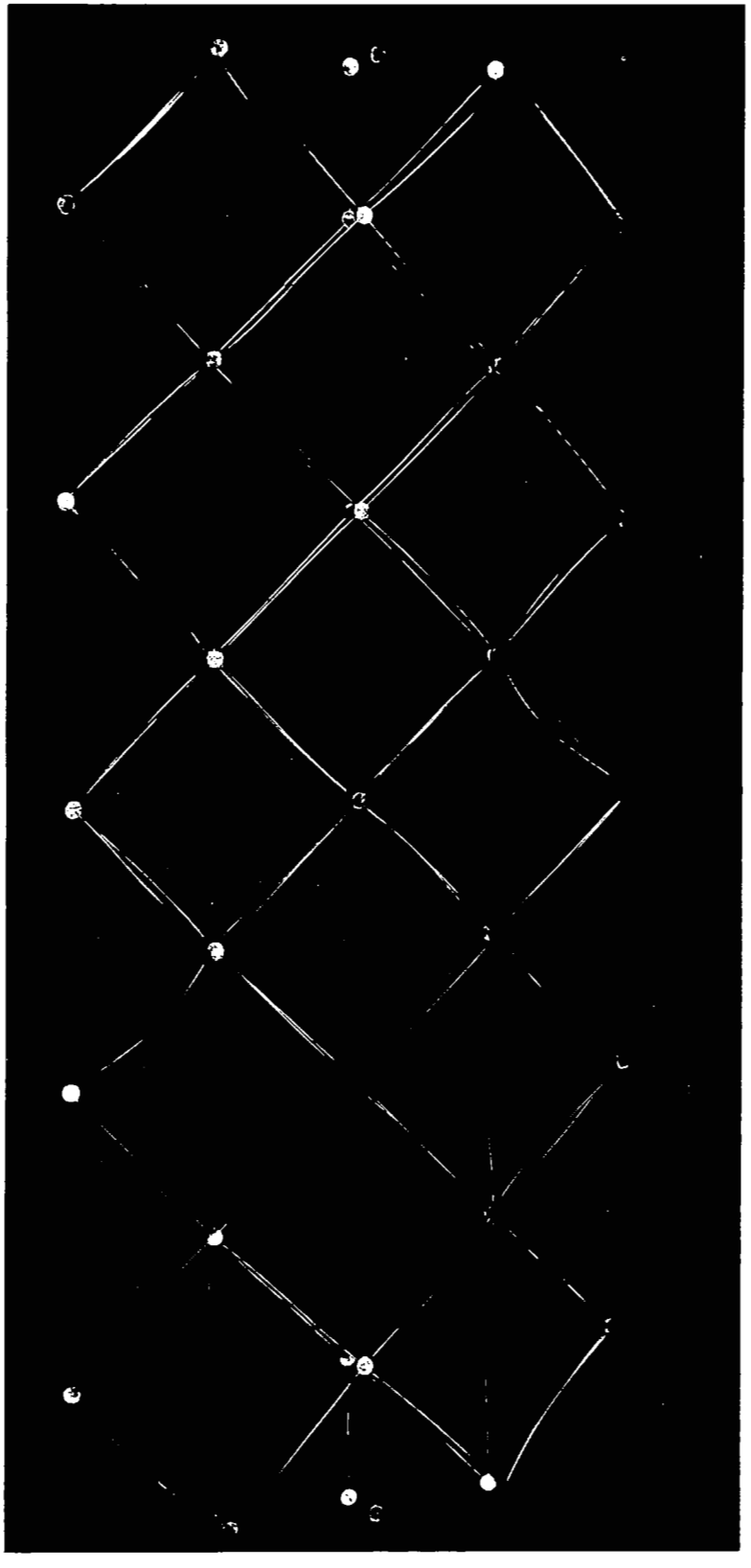

Figure 7. Test Segment in Flattened Configuration

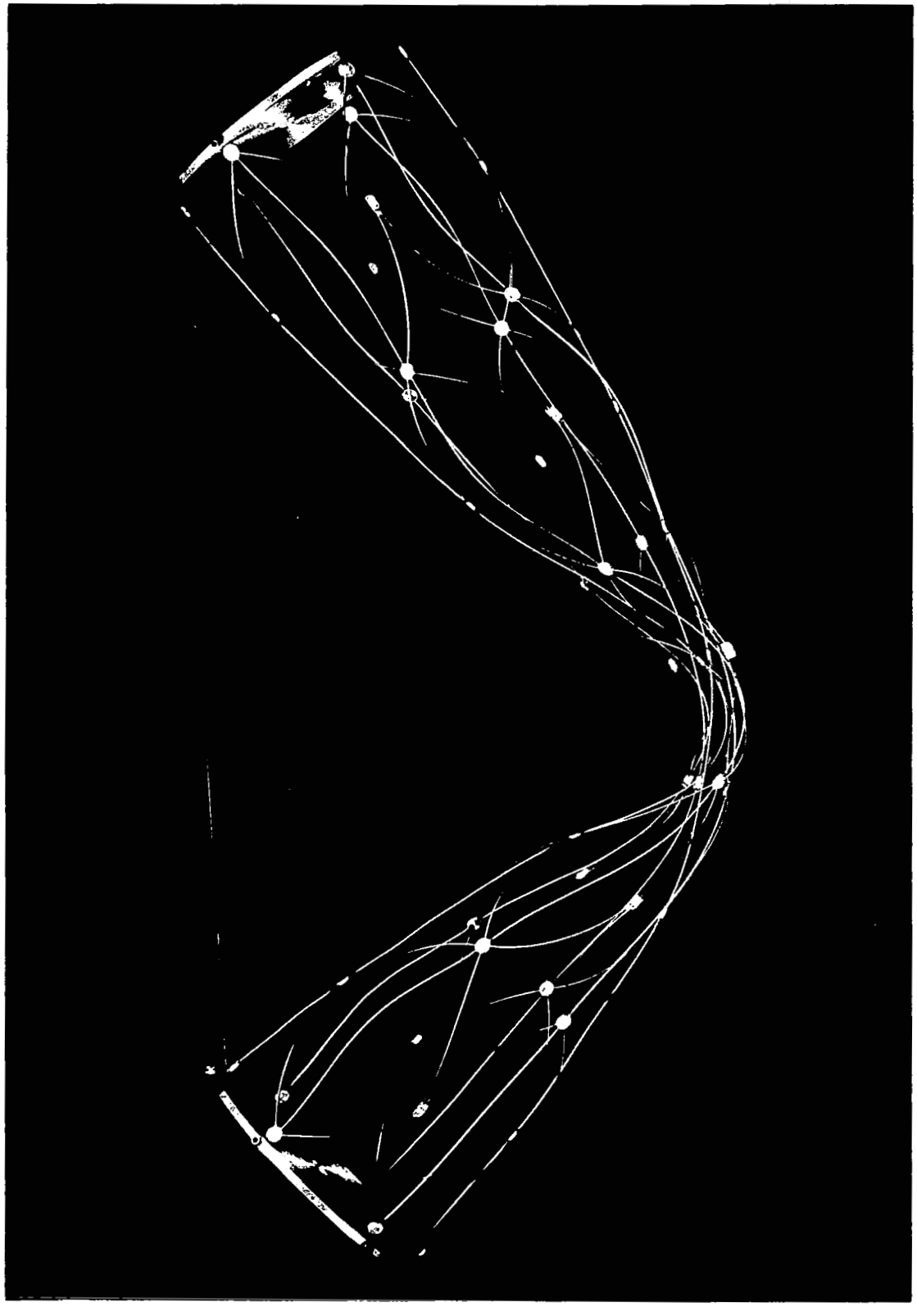

Figure 8. Test Segment in Flattened and Partly Coiled Configuration

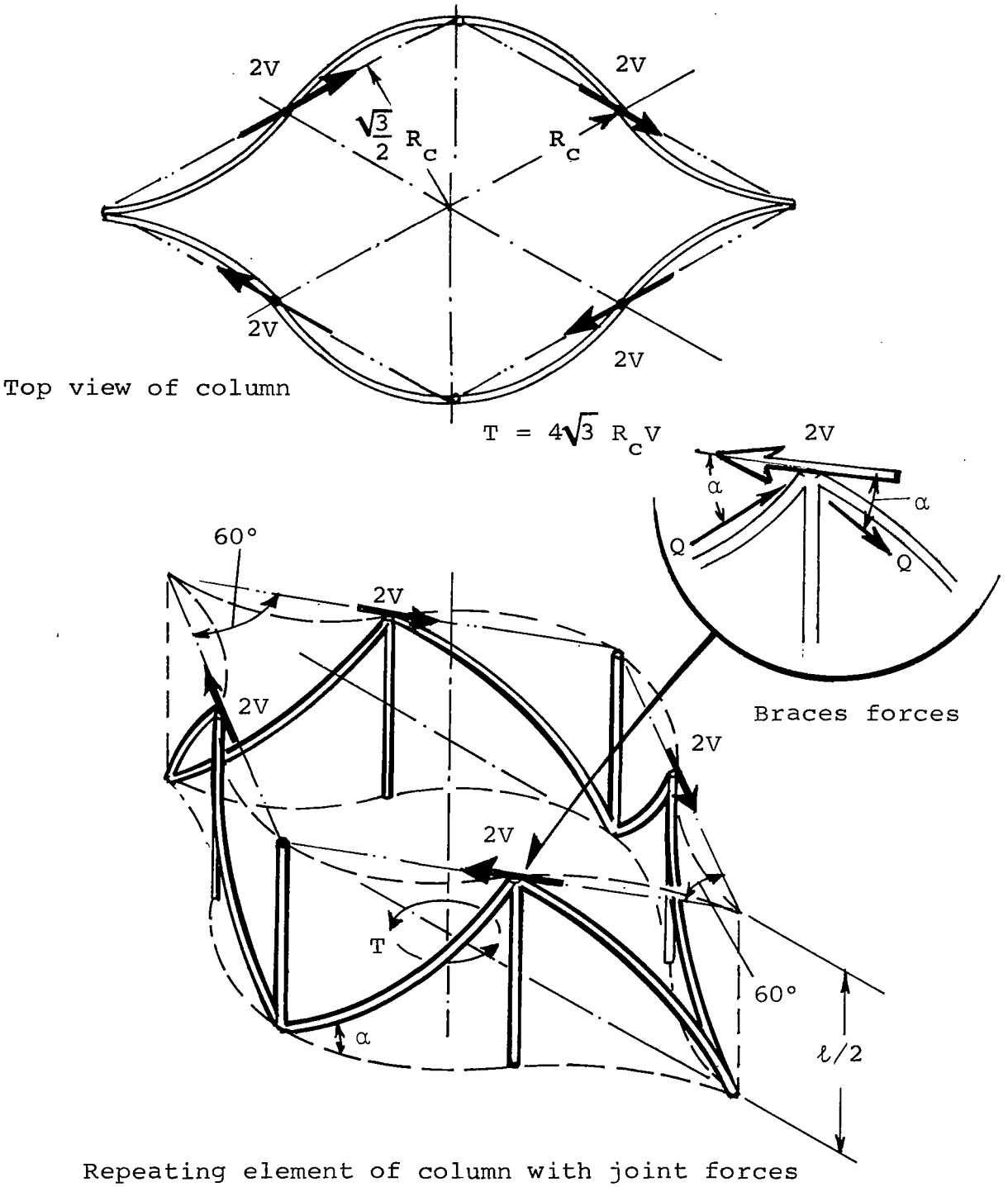

Figure 9. Schematics of Column under Applied Torque and Internal Reactions

APPENDIX

AXIAL STIFFNESS OF BRACES

When torque is applied to the column, the braces which helix in one direction will be compressed while those which helix in the other will be tensioned. Since the shape of the helical braces between intersections is circular, they will bend in reaction to these tensile and compressive forces, tending to amplify the initial radial deflections when compressed, and to diminish them when tensioned. It is the purpose of the present analysis to determine the effective axial stiffness of the braces under these conditions.

The radial deflections of each set of helical braces, those tensioned or those compressed, will be symmetric about their intersections with the center longerons and about column-edge intersections. The deflections, however, will be asymmetric about their intersections with the side longerons. Therefore, the boundary conditions used in the following analysis of a single brace segment are that one end is fixed and the other is free to rotate. It is assumed that there is no radial displacement of the intersections because radial components of the tensile and compressive forces in the brace are null at their intersections.

The axial stiffness of the helical braces is therefore analyzed in accordance with the following sketch

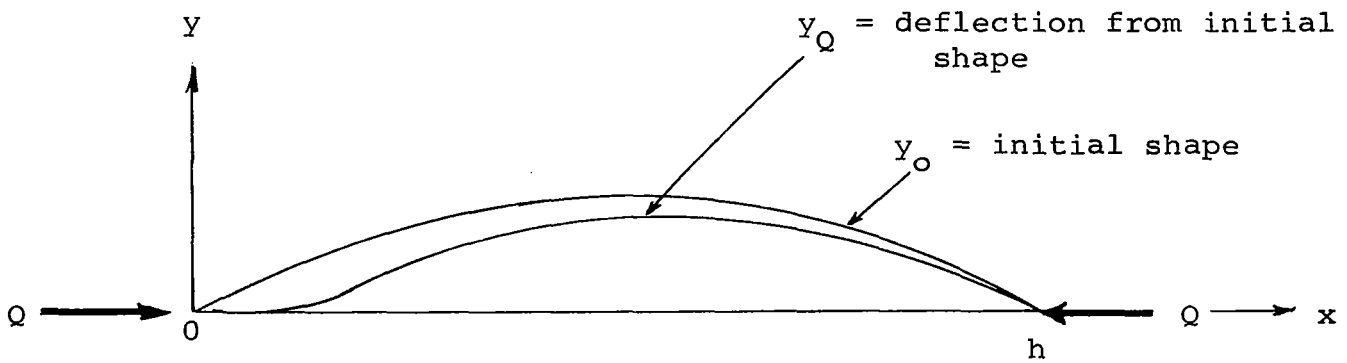

Boundary conditions:

$$y_Q(o) = y_Q'(o) = 0 \qquad \text{(A-1)}$$

$$y_Q(h) = y_Q''(h) = 0 \qquad \text{(A-2)}$$

Deflections and Boundary Conditions for Braces

Equilibrium conditions for the braces are derived from the following sketch

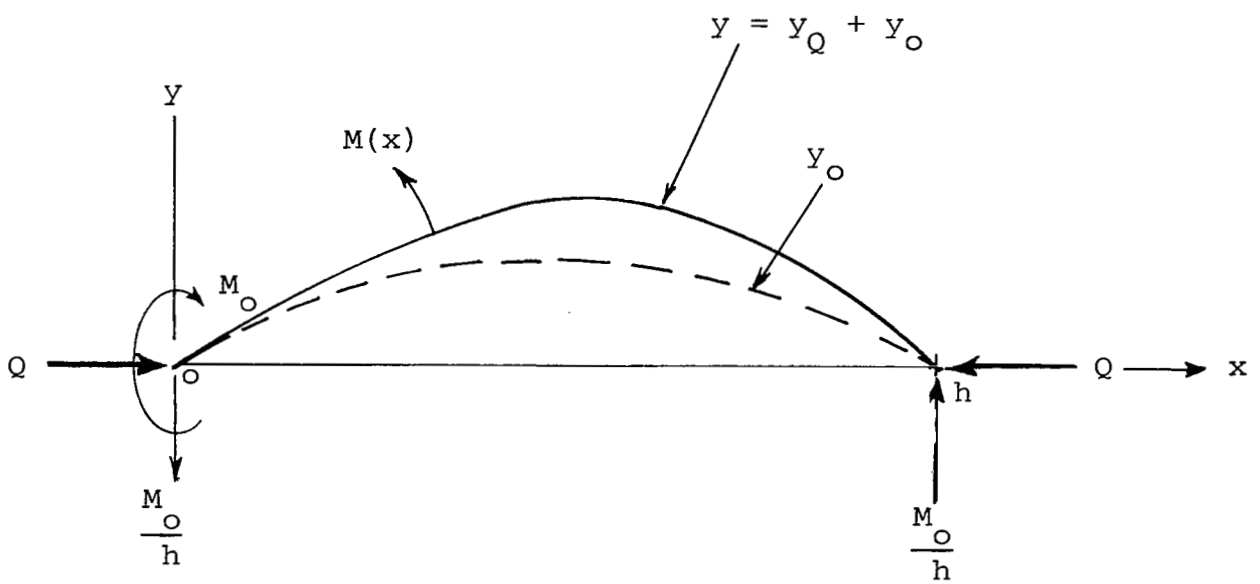

Forces on Braces

Equilibrium of moments requires that

$$M(x) + Q\,y = M_o - M_o \frac{x}{h} \qquad \text{(A-3)}$$

since

$$M(x) = EI\,y_Q'' \qquad \text{(A-4)}$$

and

$$y = y_Q + y_o \tag{A-5}$$

Equation (A-3) becomes

$$EI\, y_Q'' + Q\,(y_Q + y_o) = M_o\,(1 - \frac{x}{h}) \tag{A-6}$$

The initial circular shape of the brace is approximated as a parabola

$$y_o = 4H \frac{x}{h}\,(1 - \frac{x}{h}) \tag{A-7}$$

Therefore, the complete solution to the differential equation of equilibrium (A-6) is

$$y_Q = A \sin\lambda x + B \cos\lambda x + Cx^2 + Dx + E \tag{A-8}$$

where

$$\lambda^2 = \frac{Q}{EI} \tag{A-9}$$

By substituting the above relationships for y_Q and y_o in the differential equation, equating coefficients of like powers of x, and imposing boundary conditions (A-1), the coefficients in the solution are determined as

$$A = \frac{M_o h^2}{EI} \quad \frac{1}{(h\lambda)^3} + \frac{4H}{h\lambda} \tag{A-10}$$

$$B = \frac{1}{(h\lambda)^2} \left(8H - \frac{M_o h^2}{EI} \right) \tag{A-11}$$

$$C = \frac{4H}{h^2} \tag{A-12}$$

$$D = -\frac{4H}{h} - \frac{1}{h^3 \lambda^2}\left(\frac{M_o h^2}{EI}\right) \tag{A-13}$$

$$E = -\frac{1}{(h\lambda)^2}\left(8H - \frac{M_o h^2}{EI}\right) \tag{A-14}$$

From $y_Q(h)$ boundary condition and the above coefficients, the boundary moment, M_o, is determined as

$$\frac{M_o h^2}{EI} = \frac{4H\,(2 - 2\cos\lambda h - \lambda h \sin\lambda h)}{\frac{\sin\lambda h}{\lambda h} - \cos\lambda h} \tag{A-15}$$

As a result of these deflections of the braces, the relative axial displacements of their ends will be

$$\delta = \frac{1}{2}\int_o^h \left[(y_Q' + y_o')^2 - (y_o')^2\right] dx$$

or

$$\delta = \frac{h}{2}\int_o^1 \left[(y_Q')^2 + 2y_Q'\, y_o'\right] d\,\bar{x} \tag{A-16}$$

where

$$\bar{x} = \frac{x}{h} \tag{A-17}$$

The particular stiffness sought is the slope of the curve representing load versus end displacement of the brace when the applied end load is much smaller than its critical value. This stiffness will then be accurate in representing the initial reaction of the braces to either tension or compression. The stiffness is formulated as

$$S = \left(\frac{d\delta}{dQ}\right)^{-1} \tag{A-18}$$

for

$$Q << Q_{CR} \tag{A-19}$$

Therefore, the required stiffness is found as the following differential of Equation (A-16)

$$S^{-1} = \lim_{Q \to 0} \frac{d\delta}{dQ}$$

$$= \frac{\pi^2}{Q_{EU}} \left[\lim_{(\lambda h)^2 \to 0} \left(\frac{d\delta}{d(\lambda h)^2} \right) \right] \tag{A-20}$$

Note that

$$(\lambda h)^2 = \frac{\pi^2 Q}{Q_{EU}} \tag{A-21}$$

where

$$Q_{EU} = \frac{\pi^2 EI}{h^2} \tag{A-22}$$

The differential indicated in Equation (A-20) is

$$\frac{d\delta}{d(\lambda h)^2} = h \int_o^1 (y_Q' + y_o') \frac{dy_Q'}{d(\lambda h)^2} \, d\bar{x} \tag{A-23}$$

The limits as $(\lambda h)^2 \rightarrow 0$ of the derivatives indicated in Equation (A-23) were evaluated as follows from the foregoing solution of the equilibrium equation:

$$\lim_{(\lambda h)^2 \rightarrow 0} y_Q' = 0 \tag{A-24}$$

and

$$\lim_{(\lambda h)^2 \rightarrow 0} \frac{dy_Q'}{d(\lambda h)^2} = \frac{H}{h} \bar{x} \left(1 - \frac{5}{2} \bar{x} + \frac{4}{3} \bar{x}^2\right) \tag{A-25}$$

The derivative of y_o' is simply

$$y_o' = \frac{4H}{h} (1 - 2\bar{x}) \tag{A-26}$$

Therefore, S is found by performing the required integration as

$$S = \frac{5\ EI}{H^2\ h} \tag{A-27}$$